17th World Conference on Earthquake Engineering, 17WCEE
Sendai, Japan - September 13th to 18th 2020

Automated Modeling of Virtual Structures using Hysteresis Loop Analysis

C. Zhou[1], J.G. Chase[2], G.W. Rodgers[3]

[1] *Post-doctoral Fellow, University of Canterbury, cong.zhou@canterbury.ac.nz*
[2] *Distinguished Professor, University of Canterbury, geoff.chase@canterbury.ac.nz*
[3] *Professor, University of Canterbury, geoff.rodgers@canterbury.ac.nz*
…

Abstract

Seismic damage is a major risk in seismic zones, and may have a significant impact on the overall health or state of the structure, which can increase the potential risk of building collapse and loss of lives in an aftershock or new event in the future. Structural health monitoring(SHM) provide damage detection and localization, but not a means of answering subsequent questions concerning immediate or long-term damage mitigation, risk, or safety in re-occupancy. Extending SHM from a damage monitoring role into a more comprehensive predictive digital model for forecasting structural performance and assessing risk of collapse would provide significant benefit in optimizing decision-making and reducing uncertainty. This work presents an automated modeling approach using machine learning to translate hysteresis loop analysis (HLA) SHM results into nonlinear computation models for damage assessment and collapse prediction. The computational model for creating digital clones are based on a new identifiable smooth hysteretic models able to capture essential dynamics, deterioration of nonlinear structures and predict collapse.

A proof of concept case study is conducted to validate the accuracy and robustness of the automated modeling method in identifying model parameters for a three-story nonlinear numerical structure, where the exact values are known in the presence of 10% root mean square (RMS) noise. The identification errors for 12 model parameters are within 4.5%, and predicted response using the identified model parameters show a good match with the true response with the cross correlation coefficient $R_{corrcoef}$ greater than 0.96 for all stories. Performance of the proposed method in real world application is finally validated using a full scale three-story apartment building tested in E-defence facility in Japan. The predicted response using the identified digital clones also match well to the measured displacement response with the average $R_{corrcoef}$ of 0.92 for the real building. The overall results clearly indicate the ability of the proposed automated modeling approach to create an accurate digital clone for further analysis of risk of damage and collapse with incremental dynamic analysis (IDA).

Finally, the overall approach of creating digital clone and further implementing IDA are automated without requiring skilled engineering experience and input, thus taking SHM from a tool providing data into automated prediction analysis by "cloning" the structure using computational modelling, which in turn allows optimised decision making using existing risk analyses and tools.

Keywords: digital clones; automated modeling; structural health monitoring; Hysteresis loop analysis; HLA

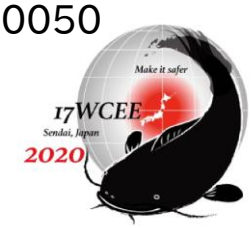

1. Introduction

Seismic damage is a major risk in seismic zones with significant follow-on social and economic impacts, and the resulting local damage may have a great impact on the overall health or state of the structure, which can increase the potential risk of building collapse and loss of lives in an aftershock or new event in the future. Therefore, post-earthquake assessment of damage and vulnerability to aftershocks based on a nonlinear dynamic analysis is considered essential to account for the evolution of material behaviours and structural properties under varying dynamic loads.

Structural health monitoring (SHM) provides methods to detect, localise, and quantify damage after major events. However, it does not provide a ready, quantified means of assessing the ongoing safety of a structure or risk of collapse, as well as any need for immediate or longer term reinforcement or repair. Therefore, a computational model made from the SHM results, and existing building data or/and reasonable surrogates, would enable further analyses to significantly enhance decision-making. However, model creation can be complex, time consuming, and require significant human input. Hence, an automated or semi-automated means of turning SHM results into actionable, reasonably accurate computational models would provide potentially significant benefit. More critically, automated model creation would enable dynamic assessment, potentially also automated, within minutes or hours, providing better data to optimise decision and reduce uncertainty.

To implement automated modelling predictions, an identifiable smooth hysteretic nonlinear model is proposed based on the Bouc-Wen model due to its ability to capture a wide range of hysteretic behaviours [1, 2]. The original Bouc-Wen model is widely used to achieve a good match of experimental data from hysteretic systems by adjusting the model parameters to minimize the error between the input data and model output. However, the model parameters have proven mathematically redundant, which might lead to an identical response with a multiplicity of parameters selection [3, 4]. Therefore, a modification is applied to the Bouc-Wen model to obtain a simplified hysteretic model with identifiable physical parameters.

A parameter identification method is developed using support vector machines (SVMs) and hysteresis loop analysis (HLA) SHM results to identify the model parameters of the proposed nonlinear predictive model for a three-story building structure tested on the E-defence shake table in Japan [5]. Support vector machines (SVM) is a machine learning technique solving a convex quadratic optimization equation for nonlinear problems, thus avoiding the local minimum issues with neural networks [6]. Therefore, the use of SVM with available SHM results converts the identification of a nonlinear system to a relatively robust pattern recognition problem, avoiding the divergence issues in the traditional methods of nonlinear optimization [7].

The primary goal of this work is a nonlinear structure model able to predict the response of subsequent nonlinear events to enable much greater detail in post event decision making. The proposed automated modelling method is validated against a numerically simulated structure with added noise and real experimental data from a full scale 3 story-building. Performance of the identified model in capturing the essential dynamics and predicting responses to future nonlinear events is assessed by cross correlation coefficients between the measured and reproduced response with the identified model.

2. Methods

2.1 differential hysteretic model

The dynamic equation of motion for a multi-degree-of-freedom nonlinear system subjected to earthquake excitations can be described:

$$\boldsymbol{F}(t) = -\mathbf{M}\mathbf{I}\ddot{x}_g(t) - \mathbf{M}\ddot{\mathbf{X}}(t) - \mathbf{C}\dot{\mathbf{X}}(t) \tag{1}$$

where $\ddot{x}_g$ is the input ground accelerations, $\ddot{\mathbf{X}}$ and $\dot{\mathbf{X}}$ are vectors of structural accelerations and velocities, $\mathbf{M}$ and $\mathbf{C}$ are mass and damping matrices, respectively. $F(t)$ is the time-varying restoring force vector, and can be decoupled to the hysteretic restoring force $f(t)$ for each story/dof in HLA [5, 8]:

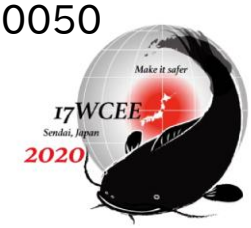

$$f_i(t) = \sum_{j=i}^{ndof} \boldsymbol{F_j}(t) \tag{2}$$

where the hysteretic restoring force $f(t)$ is assumed to comprise a linear spring and a hysteretic component in parallel [2]:

$$f(t) = \alpha k_0 x + (1-\alpha) k_0 z \tag{3}$$

where k_0 is the initial stiffness, α is the post-yielding ratio, x is the inter-story displacement, and z is the hysteretic displacement. The differential form of Equation (3) can be expressed:

$$df = \alpha k_0 dx + (1-\alpha) k_0 dz \tag{4}$$

Dividing dx on both sides of Equation (4), the instantaneous stiffness $k(t)$ can be obtained:

$$k(t) = \frac{df}{dx} = \alpha k_0 + (1-\alpha) k_0 \frac{\dot{z}}{\dot{x}} \tag{5}$$

where $\frac{\dot{z}}{\dot{x}}$ is defined in the original Bouc-Wen model:

$$\frac{\dot{z}}{\dot{x}} = \frac{\mathrm{A} - (\beta sign(\dot{x}z) + \gamma)|z|^p}{\eta} \tag{6}$$

where A, β, λ, p are dimensionless loop parameters, sign is the signum, and η is the degradation function controlled by $\delta\eta$ and total dissipated energy $\varepsilon(t)$:

$$\eta = 1 + \delta_\eta \varepsilon(t) \tag{7}$$

$$\varepsilon(t) = (1-\alpha)\frac{k}{m}\int_0^t z\dot{x}dt \tag{8}$$

The parameter A in Equation (6) has been found a redundancy parameter and can be fixed to one without changing the efficacy of the model [4]. The maximum value of z can be calculated by setting Equation (6) to zero, yielding:

$$z_{max} = \left(\frac{1}{\beta+\gamma}\right)^{1/p} \tag{9}$$

where z_{max} indicates the start of purely plastic phase, and can be defined by a yielding displacement parameter dy to account for the elastic-plastic performance in the hysteretic model. In addition, the loading and unloading slopes for steel and concrete structure are nearly in parallel if degradation is not considered [9, 10], which yields another constraint $\beta=\gamma$. Thus, Equation (5) can be rewritten:

$$k(t) = \alpha k_0 + (1-\alpha) k_0 \frac{1 - 0.5(sign(\dot{x}z)+1)\left|\frac{z}{dy}\right|^p}{\eta(t)} \tag{10}$$

Therefore, the unknown parameters for Equation (10) included k, k_0, α, dy, p, δ_η, where k is the structural stiffness, k_0 is the initial stiffness, α is the post-yielding ratio, dy is the yield displacement, p is the smoothness from elastic to plastic state and δ_η controls how the stiffness changes due to energy dissipation.

2.2 Model parameter identification

To identify the model parameters in Equation (10), the elastic stiffness $k_e(t)$ can be approximated by setting hysteretic displacement z=0 in Equation (10), yielding:

$$k_e(t) = \alpha k_0 + (1-\alpha) k_0 \frac{1}{\eta(t)} \tag{11}$$

The stiffness vectors $k_e(t)$, $k(t)$, and k_0 can be directly obtained from HLA results [5].

Combining Equations (7), (8) and (11) gives:

$$y = \delta_\eta u \tag{12}$$

$$y = \frac{m(k_0 - k_e)}{(1-\alpha)k_e(k_e - \alpha k_0)};\ u = \int_0^t z\dot{x}dt \tag{13}$$

Thus, the degradation coefficient δ_η can be calculated using regression analysis:

$$\delta_\eta = \frac{\sum_{i=1}^{N} u_i y_i}{\sum_{i=1}^{N} u_i u_i} \tag{14}$$

In addition, for each half cycle in HLA, Equations (11)-(12) can give:

$$\hat{y} = d_y \hat{u} \tag{15}$$

$$\hat{y} = |z|;\ \hat{u} = \left(\frac{(k_e - k)}{(k_e - \alpha k_0)}\right)^{1/p} \tag{16}$$

Similar to Equation (14), the yield parameter *dy* can also be calculated:

$$d_y = \frac{\sum_{i=1}^{N} \hat{u}_i \hat{y}_i}{\sum_{i=1}^{N} \hat{u}_i \hat{u}_i} \tag{17}$$

Finally, the curve transition parameters α and p are identified using a SVM method. In particular, each half cycle is divided into n segments with feature v_i (i=1,2,…,n) calculated:

$$v_i = \frac{k_e(i) - k(i)}{k_0} \tag{18}$$

The calculated features within each half cycle are concatenated to train multi-class SVM models for various shapes of simulated half cycles with controlled α and p values in the proposed hysteretic model. The new feature vector from real data can then tested using the trained SVM model to identify the best match of α and p.

The modified SMO algorithm is used to train the SVM model [11]. In addition, a Gaussian Radial Basis Function (RBF) kernel is employed to transform the feature vector v into a nonlinear space due to its strong learning ability in nonlinear cases [12]:

$$K(v_i, v_j) = \exp\left(-\frac{\|v_i - v_j\|^2}{2\sigma^2}\right) \tag{19}$$

where σ is the kernel width, and a lower value leads to a more complex model fitting and allows for a smaller variance, thus less generalization, in measuring similarity.

To identify a range of α and p parameters in this study, a Decision Directed Acyclic Graph (DDAG) method is conducted to form a binary learning architecture with $m(m\text{-}1)$ nodes for the m-class SVM [13].The range of the post-yield ratio α is [0, 1], where α=0 indicates a total hysteretic behaviour and α=1 represents a purely elastic linear structure. However, the maximum range of α_{max} is restricted by the constraint $(k_e\text{-}\alpha k_0)>0$ in Equation (13) to ensure a positive solution for δ_η. Thus, the selected range for α is α_{min}=0 and α_{max} =inf(k_e/k_0), where inf is the infimum maximum value.

To ensure a unique solution, the inequality condition $p\geq1$ is also applied [14]. In addition, due to its low sensitivity among the model parameters, p is commonly fixed to be p=1 or 2 in most of identification methods [15-17]. Hysteresis loops with p>3 are closer to a bilinear model, where the smoothness of the transition part

is hardly changed with the change of p for p>3 [18]. Therefore, the selected range for p is constrained to p_{min}=1 and p_{max}=3.

Finally, an inner loop is operated to update the selection of α and p with a smaller range, and an outer loop is then applied to the updated range to identify and calculate the model parameters of α, p, δ_η and dy for the modified hysteretic model.

3. Proof of concept analysis

3.1 Numerical simulated structure

A numerical model structure is first simulated for a 3-story steel moment resisting frame (SMRF) building tested in the E-defence shake table in Japan [5] using the Runge-Kutta integration method with added 10% RMS noise to both ground and structural accelerations. A sampling rate of 200Hz is adopted to match the true measurement frequency. The velocities and displacements are obtained by direct and double integration of measurement accelerations after a band pass filtering.

The model parameters α, dy, p, δ_η, of the numerical structure are defined in Table 1 for all three stories. The weight and stiffness for each story are m1=m2=171.85kN, m3=90kN, k1=1.94e4N/mm, k2=1.65e4N/mm and k3=1.37e4N/mm, which are the same as reported for the experimental test building. The peak ground acceleration (PGA) for the input earthquake in this numerical case study is 0.62g. The time history of the input earthquake is shown in Fig. 1. Table 1 summarizes the model parameters employed.

Table 1 – Model parameters for the proof-of-concept numerical structure

model parameters	1st story	2nd story	3rd story
α	0.23	0.17	0.12
p	2.5	1.5	1.9
d_y	7	6	3
δ_η	0.7	0.66	1.54

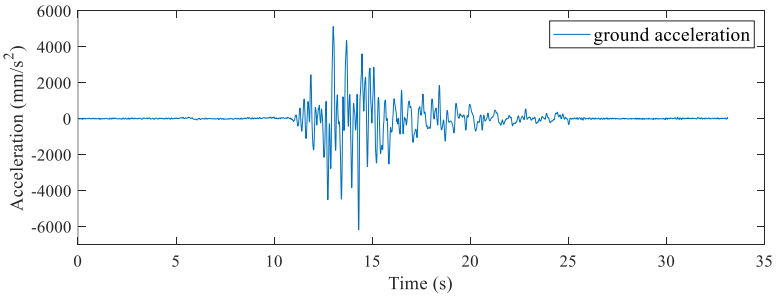

Fig. 1– Time history of the input earthquake

3.2 Number of training samples for SVM

Fig. 2 compares the test accuracy with different numbers of training samples (100, 300, 500, 700, 1000, 1500 and 2000) for training the SVM model. Clearly, the test accuracy is increasing with the increasing number of training samples for both parameters α and p, as should be expected. Moreover, the test accuracy for α shows

better results than for p at the same number of samples, indicating α is a more sensitive parameter. However, the test accuracy of α and p are both greater than 94% when the number of training samples are greater than 1500, which can be done with ~30minutes on a 16GB Intel Core i-7 machine.

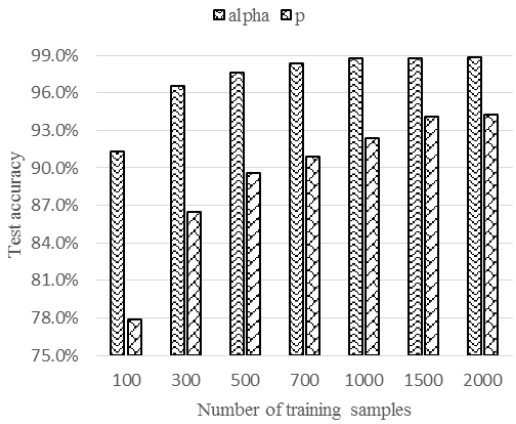

Fig. 2– Effect of number of training samples on the test accuracy for identifying α and p

3.3 Identification for the numerical structure

The HLA SHM results for $k_e(t)$, $k(t)$, and k_0 yield the selected ranges of α are [0, 0.6], [0, 0.6], [0, 0.55] for the first, second and third story, respectively. Thus, the target values of y for training the SVM model in the inner loop are set based on the identified values of α and p with a coarser resolution as listed in Tables 2 and 3. Each target value corresponds to a range of 0.05 for α in Table 2, and 0.04 for p in Table 3.

Table 2 – Target values of y for α in the inner loop

target value	1	2	3	4	5	6
α value	0~0.05	0.05~0.10	0.10~0.15	0.15~0.20	0.20~0.25	0.25~0.30
target value	7	8	9	10	11	12
α value	0.30~0.35	0.35~0.40	0.40~0.45	0.45~0.50	0.50~0.55	0.55~0.60

Table 3 – Target values of y for p in the inner loop

target value	1	2	3	4	5
p value	1.0~1.4	1.4~1.8	1.8~2.2	2.2~2.6	2.6~3.0

The predicted target values for α using the trained SVM model are 5, 4 and 3 for the first, second, and third story, respectively, corresponding to the α range of [0.20~0.25], [0.15~0.20] and [0.10~0.15], respectively. Thus, the range of α are updated considering the boundary crossing effect with the identified smaller range [0.15, 0.3], [0.10, 0.25] and [0.05, 0.20] for each story with new target values assigned for a finer resolution. The new target values are y=1,2,…,15 for each story with each value representing $\Delta\alpha$=0.01. Similarly, the predicted target values for p are 4, 2 and 3 for the first, second, and third story, respectively. The new ranges for p are then updated to [1.8, 3.0], [1.0, 2.2] and [1.4, 2.6] with Δp=0.1 for the new target values.

Finally, the values of α, p, dy, δ_η are identified in the outer loop, and compared to the true values in Table 4. The identification errors for all 12 parameters are smaller than 4.3% with average error of 2.8%, which indicates a very accurate identification with 10% RMS added noise in the simulated data.

Displacement responses of each story are also compared between the true simulated response and the predicted response using the identified parameters, as shown in Fig. 3. The cross correlation coefficient $R_{corrcoef}$ used to measure the similarity of two series are calculated for the response in Fig. 3, and the values of $R_{corrcoef}$ for all stories are greater than 0.96, which thus shows a good match between the true and identified response trajectories over time.

Table 4 – Identified model parameters compared to the true values

model parameters	story	identified	true	error
α	1st	0.225	0.23	2.2%
	2nd	0.175	0.17	2.9%
	3rd	0.125	0.12	4.2%
p	1st	2.55	2.5	2.0%
	2nd	1.45	1.5	3.3%
	3rd	1.95	1.9	2.6%
δ_η	1st	0.73	0.7	4.3%
	2nd	0.68	0.66	3.0%
	3rd	1.54	1.54	0.0%
d_y	1st	6.7	7	4.3%
	2nd	5.9	6	1.7%
	3rd	3.1	3	3.3%

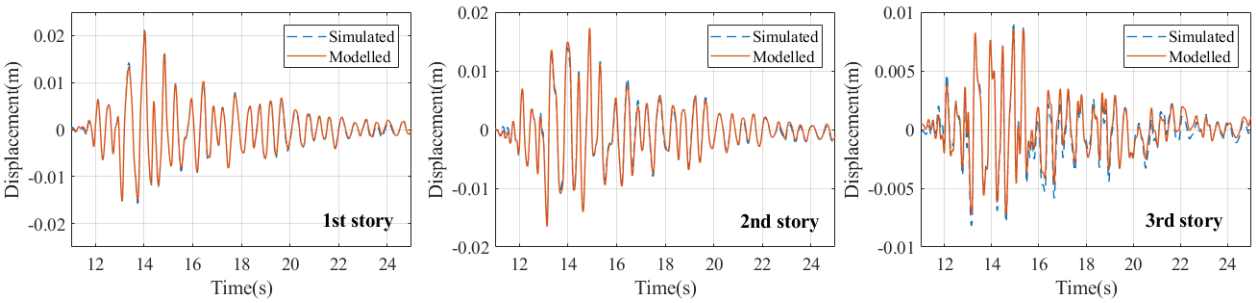

Fig. 3 – Comparing the true and predicted response for the numerical structure

4. Experimental results

Hysteresis loops are constructed and stiffness evolutions are identified in HLA algorithm for the three floors of the full scale 3-story building. Model parameters are then identified for the developed model using the proposed SVM algorithm. The dynamic responses are finally predicted using the identified nonlinear hysteretic model to compare with the true measured response, as shown in Fig. 4. The calculated cross correlation coefficients $R_{corrcoef}$ between the measured and replicated response in Fig.4 are 0.94, 0.92, 0.89 for the first, second and third story, respectively, again showing a good prediction accuracy using the identified virtual model. Moreover, the predicted stiffness evolution also match the HLA SHM results well with average error of 2.1% in Fig. 5, thus providing a good cross-validation between the prediction and HLA SHM results.

It is important to note the developed baseline model is an approximation of the physical system, which does not necessarily represent the exact ground truth due to the model uncertainty and mathematical assumptions [8]. Thus, the response comparison shows there may be some differences in the chosen baseline model and the actual structure, as should be expected. However, the results show a significant correlation despite the difference in peak values and trajectories, which thus validate the hysteretic model with the identified parameters successfully captures the essential dynamics and stiffness degradation of the test building. A more complex model might yield a more accurate results, while it would require much longer time to process, and may also suffer the identifiably and model mismatch issues. There is a potential trade off and compromise amongst increasing complexity, increasing accuracy, and simplicity / automation, while in this case the developed model and identification algorithm have proven good estimation with the algorithm implemented in an automated fashion.

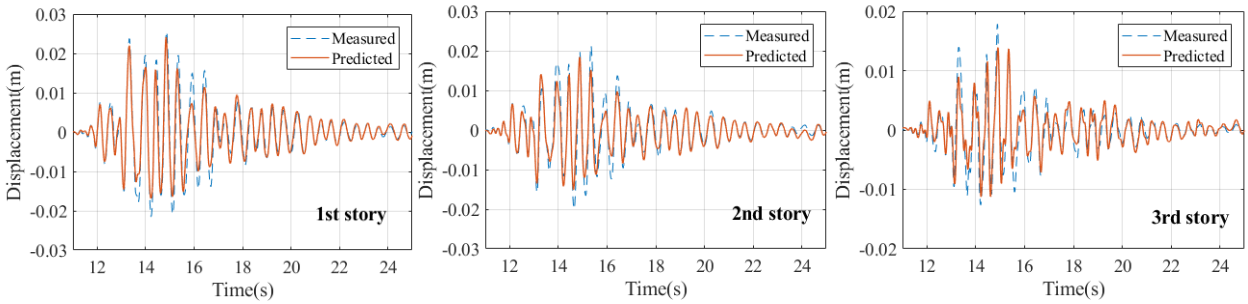

Fig. 4 – Comparing the true and predicted response for the experimental structure

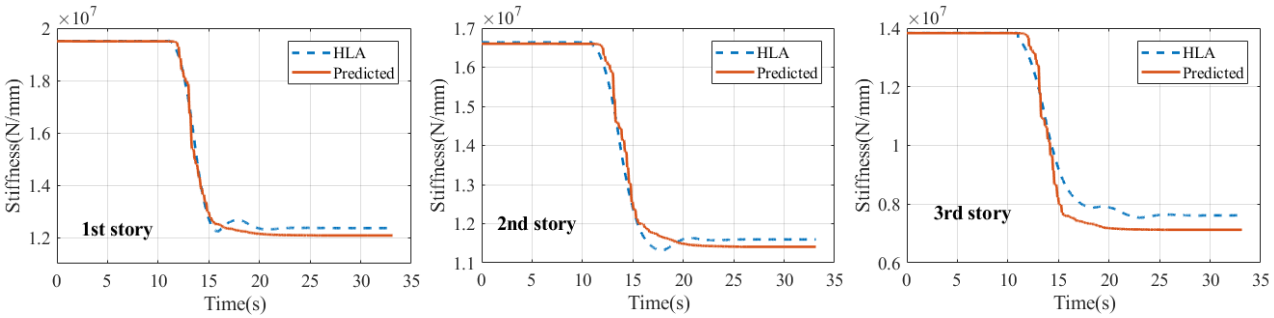

Fig. 5 – Comparing the HLA and predicted stiffness degradation for the experimental structure

5. Conclusion

This work aims to create a nonlinear hysteretic model for use with model-free structural health monitoring HLA methods and SVM identification methods. The goal is to create accurate baseline models using data from SHM damage identification and localisation methods to create models suitable for further investigation and analysis on safety, damage mitigation, and thus re-occupancy. Such models would take SHM from being a tool for damage identification and extend them into further decision-making, creating far greater utility for engineers and owners, which could further spur impetus for investment in monitoring.

The results of numerical case study show the model parameters are identified with average error of 2.8% across all stories with 10% added noise, indicating the accuracy and robustness of the identification. In addition, the modelled response with the identified parameters match the true response very well with cross correlation coefficients greater than 0.96, which thus validates the capability of the proposed algorithm to accurately model the seismic response in an automated fashion. The final experimental validation further proves the efficiency and accuracy of the overall approach. More importantly, the overall modelling approach is readily automated as it required no human input, thus suitable for a long-term in-site monitoring, considering its good or high accuracy.

6. Acknowledgements

The authors acknowledge Dr. Chikara Iihoshi and Asahi Kasei Homes Corp., Japan, for kindly providing the shake table test data.

7. References

[1] R. Bouc, Forced vibration of mechanical systems with hysteresis, Proceedings of the fourth conference on non-linear oscillation, Prague, Czechoslovakia, 1967.
[2] Y.-K. Wen, Method for random vibration of hysteretic systems, Journal of the engineering mechanics division, 102 (1976) 249-263.
[3] A. Charalampakis, V. Koumousis, A Bouc–Wen model compatible with plasticity postulates, Journal of Sound and Vibration, 322 (2009) 954-968.
[4] F. Ma, H. Zhang, A. Bockstedte, G.C. Foliente, P. Paevere, Parameter analysis of the differential model of hysteresis, Journal of Applied Mechanics, 71 (2004) 342-349.
[5] C. Zhou, J.G. Chase, G.W. Rodgers, C. Iihoshi, Damage assessment by stiffness identification for a full-scale three-story steel moment resisting frame building subjected to a sequence of earthquake excitations, Bulletin of Earthquake Engineering, 15 (2017) 5393-5412.
[6] M.A. Hearst, S.T. Dumais, E. Osuna, J. Platt, B. Scholkopf, Support vector machines, IEEE Intelligent Systems and their applications, 13 (1998) 18-28.
[7] J.A. Suykens, Nonlinear modelling and support vector machines, Instrumentation and Measurement Technology Conference, 2001. IMTC 2001. Proceedings of the 18th IEEE, IEEE, 2001, pp. 287-294.
[8] C. Zhou, J.G. Chase, G.W. Rodgers, C. Xu, Comparing model-based adaptive LMS filters and a model-free hysteresis loop analysis method for structural health monitoring, Mechanical Systems and Signal Processing, 84 (2017) 384-398.
[9] J.R. Davis, Tensile testing, ASM international, 2004.
[10] M. Devadas, Reinforced concrete design, Tata McGraw-Hill Education, 2003.
[11] R.-E. Fan, P.-H. Chen, C.-J. Lin, Working set selection using second order information for training support vector machines, Journal of machine learning research, 6 (2005) 1889-1918.
[12] B. Scholkopf, K.-K. Sung, C.J. Burges, F. Girosi, P. Niyogi, T. Poggio, V. Vapnik, Comparing support vector machines with Gaussian kernels to radial basis function classifiers, IEEE transactions on Signal Processing, 45 (1997) 2758-2765.
[13] J.C. Platt, N. Cristianini, J. Shawe-Taylor, Large margin DAGs for multiclass classification, Advances in neural information processing systems, 2000, pp. 547-553.
[14] F. Ikhouane, V. Mañosa, J. Rodellar, Dynamic properties of the hysteretic Bouc-Wen model, Systems & control letters, 56 (2007) 197-205.
[15] M. Ismail, F. Ikhouane, J. Rodellar, The hysteresis Bouc-Wen model, a survey, Archives of Computational Methods in Engineering, 16 (2009) 161-188.

[16] L. Jeen-Shang, Z. Yigong, Nonlinear structural identification using extended Kalman filter, Computers & Structures, 52 (1994) 757-764.
[17] S.K. Kunnath, J.B. Mander, L. Fang, Parameter identification for degrading and pinched hysteretic structural concrete systems, Engineering Structures, 19 (1997) 224-232.
[18] H. Zhang, G.C. Foliente, Y. Yang, F. Ma, Parameter identification of inelastic structures under dynamic loads, Earthquake engineering & structural dynamics, 31 (2002) 1113-1130.

